Joint Seismic VVAz-AVAz Inversion: A case study from offshore Abu Dhabi

L. Michou[1], O. Kirstetter[2], D. Laurencin[1], F. Ali AlJaberi[3], V. Souvannavong[1], G. Cambois[2], B. Deschizeaux[1], A. AlKaabi[3], J. Coulon[1], M. Alderei[3], T. Le Canu[1], S. Yves Anthoine[3], B. Roure[1,4], H. Kheidri[3], M. Waqas[3], S. Ahmed[3]

[1] CGG; [2] ADNOC Upstream; [3] ADNOC Offshore; [4] Parex Resources

Summary

Fracture characterisation is a key factor for reservoir production optimization. Velocity Variation with Azimuth (VVAz) and Amplitude Variation with Azimuth (AVAz) are the main technologies currently used in the industry for azimuthal anisotropy characterisation, whether it is fracture- or stress-induced, from PP seismic data. These two technologies have their respective strengths and limitations and are often used separately to predict the reservoir fracture networks. In this paper, a joint azimuthal velocity and amplitude inversion workflow is presented to characterise the fracture orientation and intensity of a Middle East offshore carbonate reservoir using a high density WAZ OBC 3D seismic survey.

Joint Seismic VVAz-AVAz Inversion: A case study from offshore Abu Dhabi

Introduction

Seismic fracture characterisation has the potential to add significant value to reservoir characterisation and management. This is especially true for carbonate reservoirs when seismic anisotropy response can be directly linked to both fracture network intensity and orientation, and therefore to permeability. Simultaneously inverting seismic azimuthal amplitude and travel time information with joint VVAz-AVAz inversion, as presented by Roure (2021), enables a more accurate characterisation of the fracture parameters. The main aspects of this innovative methodology are summarised in the first part, while the second part presents the results of a fractured carbonate case study in offshore Abu Dhabi.

Traditional azimuthal inversion approach and limitations

Kinematic and amplitude information derived from reflection seismic in different directions provides two independent attributes that can be used to characterise the horizontal transverse isotropy (HTI) medium. The kinematic anisotropy, driven by travel time or velocity variation with azimuth (VVAz), is a very robust measurement but provides low-resolution information. The amplitude versus azimuth (AVAz) analysis, performed on travel time corrected seismic data, has the advantage of providing high frequency attributes at the reservoir level for fracture characterisation. Nevertheless, this method is also highly sensitive to seismic noise, residual multiples, or azimuthal bias coming from non-isotropic acquisition settings, and as discussed in Downton (2016), AVAz modelling also suffers from a 90° ambiguity and bias due to AVA-AVAz crosstalk. For these reasons, if derived independently using either kinematic or amplitude information, anisotropic parameters are difficult to reconcile afterwards. As an alternative to this standard flow, and to reduce the solution space inherent to each method (Figure 1), a new approach, the joint VVAz-AVAz inversion process, is proposed starting from a process preserving any azimuthal misalignment.

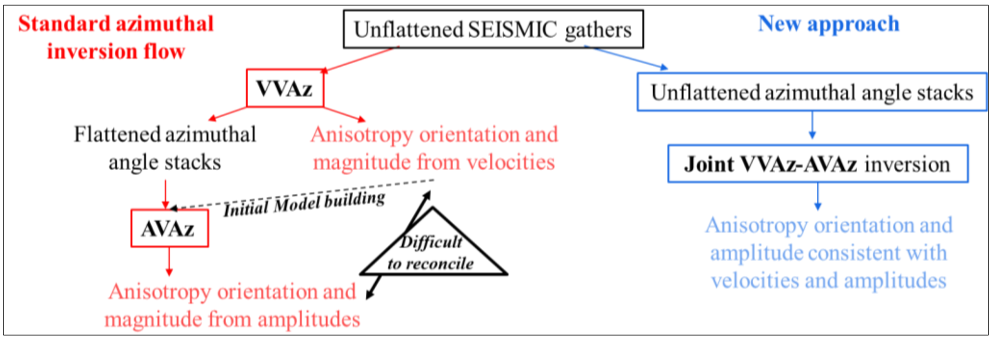

Figure 1 *Comparison of standard seismic anisotropy characterisation methods and the new approach.*

New joint azimuthal velocity and amplitude (VVAz-AVAz) inversion theory and workflow

The joint VVAz-AVAz inversion is performed using an elastic parameterisation (Vp, Vs, ρ) coupled with anisotropic parameters corresponding to the orientation, the normal and the tangential weaknesses (denoted as Φ_{sym}, Δ_N, Δ_T respectively) - described in a layered framework and following Downton and Roure (2010) AVAz modelling. The effective azimuthal velocity is derived assuming the linear slip theory using Rüger (1998) and Bakulin et al. (2000), where φ is the azimuth, $\delta^{(v)}$ and $\epsilon^{(v)}$ are the Thomsen's parameters, and g (background velocities' square ratio) and V_{fast}, related to matrix properties, are defined as:

$$V_{az}(\theta,\varphi) = V_{fast} * \left(1 + \delta^{(v)} \sin^2\theta \cos^2(\varphi - \varphi_{sym}) + \left(\epsilon^{(v)} - \delta^{(v)}\right) sin^4\,\theta\, cos^4(\varphi - \varphi_{sym})\right), \quad (1)$$

$$\text{where } \epsilon^{(v)} = -2g(1-g)\Delta_N \text{ and } \delta^{(v)} = -2g(\Delta_T + (1-2g)^2\Delta_N)$$

$$g \approx (Vs/Vp)^2 \text{ and } V_{fast} \approx Vp\sqrt{1-(1-2g)^2\Delta_N}$$

Thereby, any perturbation in the layered model (velocities, layer thickness, anisotropy) can be translated following Equation (1) into effective azimuthal velocity changes. Travel time and reflectivity changes are deduced from these azimuthal velocity variations to evaluate the modelling in a unified VVAz-AVAz framework. Group and phase velocities and angles are reconciled in this joint approach.

The workflow is described as follows. Prior to performing a joint VVAz-AVAz inversion, the rock isotropic background is first derived using a classical AVA elastic inversion. Then, a standard AVAz inversion of flattened azimuthal stacks is carried out to give a first estimation of the azimuthal parameters (Δ_N, Δ_T, Φ_{sym}). Azimuthal time shifts can then be derived from these inverted azimuthal parameters and compared to the measured azimuthal seismic time shifts: this QC allows assessing the feasibility to perform a successful joint VVAz-AVAz inversion workflow with consistent results.

The joint VVAz-AVAz inversion flow starts with an isotropic solution derived from an initial elastic AVA result, where anisotropic parameters (Δ_N, Δ_T and Φ_{sym}) are iteratively modified. Each modification is translated, using Equation (1), into a local reflectivity change and a time shift adjustment for all layers below the proposed modification. The resulting synthetic data are compared to the real seismic. This unified amplitude and time framework allows the inversion process to converge towards a solution honouring both the azimuthal amplitude reflectivity and the kinematic effects.

This cascaded inversion approach (AVA => AVAz => VVAz-AVAz) allows to minimise the crosstalk between AVA and AVAz parameters and removes the azimuthal direction 90˚ ambiguity. Moreover, thanks to the VVAz kinematic constraint, the new method gives more robust anisotropy amplitude and orientation results while keeping the local layer information. In the case of a lack of detailed rock physics information, it can be challenging to control the coupling between Δ_N and Δ_T attributes related to the fluid behaviour, crack plasticity and rugosity due to pressure waves. For now, the method enables the extraction of a robust high-frequency proxy for crack density with the Δ_T attribute, whereas the coupling of Δ_T and Δ_N is still to be studied.

Offshore Abu Dhabi Case Study

Both AVAz and joint VVAz-AVAz inversions were performed on a high-density wide azimuth 3D survey from offshore Abu Dhabi. The reservoir of interest, a late Cretaceous carbonate, is characterised by complex fracture systems, varying in intensity laterally, vertically and within and between the reservoir layers (Gibson et al., 1992). Their understanding is key to optimise hydrocarbon production. The study main objectives were to identify, using seismic data, the main fracture systems and corridors.

To assess the existence and reliability of seismic anisotropy information, a feasibility study was carried out starting with a seismic pre-conditioning flow that aimed to increase the signal-to-noise ratio and optimise the amplitude versus angle and azimuth responses. Based on the encouraging Fast to Slow velocity ratio correlation with the anisotropic gradient estimated from the seismic azimuthal amplitude variations from the Fourier Coefficient approximation (Downton and Roure, 2015), the inversion workflow was applied to further improve the vertical resolution and obtain layer properties rather than interface properties (e.g., the anisotropic gradient).

The initial tangential (Δ_T) and normal (Δ_N) weakness properties were set to zero. The initial fracture orientation was set to 30˚, based upon measurements from well information. Figure 2 illustrates the AVAz inversion results: the tangential weakness in a 2D section (a), its RMS computed over a 50 ms target interval (b) and the corresponding fracture orientation average map with a threshold selection on high tangential weakness values (c). The fracture orientation distribution is also illustrated via the azimuthal polar plot color-coded by the Δ_T amplitudes. The inversion revealed high anisotropy areas within the target interval and on the top of the structural crest, mostly within an NNE-SSW corridor. The main anisotropy direction was stable for high tangential weakness values, with few points of lower tangential weakness values rotated to a 90° value as observed on the polar plot. The normal weakness results were less stable and more difficult to interpret.

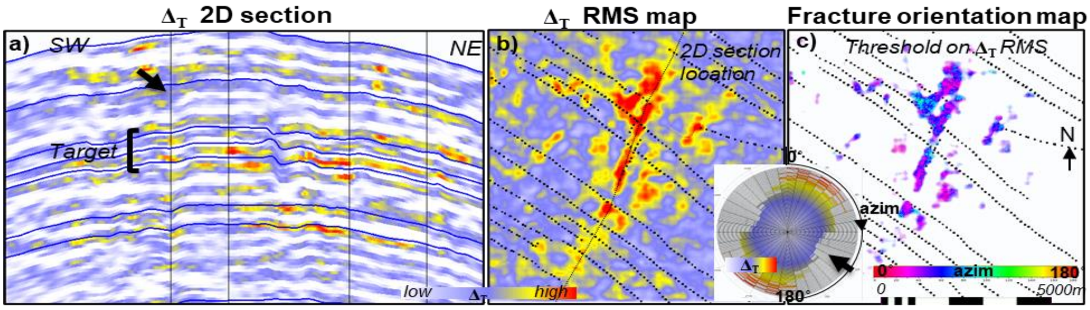

Figure 2 *AVAz inversion outputs: a) 2D tangential weakness section (ΔT), b) tangential weakness RMS map over target interval and c) average fracture orientation on target interval. The polar plot presents the tangential weakness values distribution along the azimuths. Dotted lines are major faults.*

A key AVAz inversion QC consisted of modelling the azimuthal time shifts and comparing them with the azimuthal NMO time shifts, which included overlaying seismic and synthetic data and analyzing azimuthal time shift maps. Globally, the AVAz final inversion results explained most of the azimuthal NMO time shifts (Figures 3a and 3b). Figure 3d illustrates a CMP location where the anisotropic parameters derived from the AVAz inversion tend to locally over-estimate the azimuthal time shifts observed on the real seismic data, which is improved using the VVAz-AVAz approach (Figure 3e).

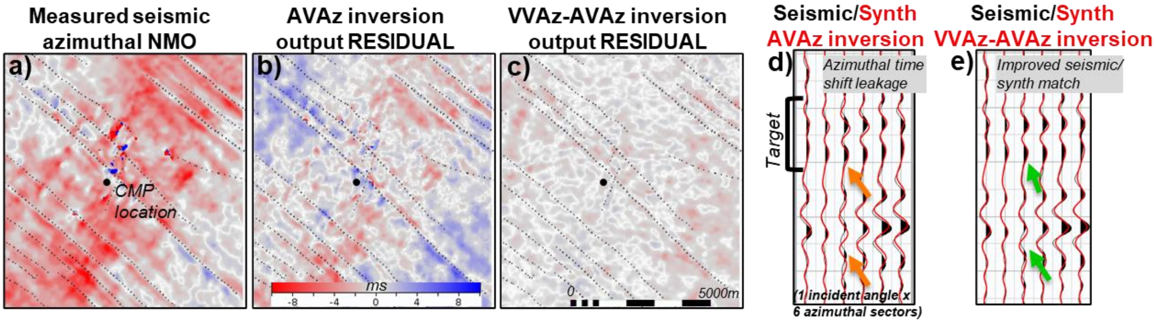

Figure 3 *Comparison of AVAz and VVAz-AVAz results. (a) to (c) represent the time shift maps in ms computed on the target between the full stack and the far azimuthal angle stack (average azimuth 135°): a) measured seismic NMO time shift, b) residuals from AVAz inversion, c) residuals from VVAz-AVAz inversion. (d) and (e): 1D view seismic azimuthal angle stacks (black) overlaid by synthetic (red).*

The joint seismic VVAz-AVAz inversion led to a stabilization of the results, with the overburden and the background anisotropy being clearly attenuated (Figure 4a). Although quantitatively the tangential weakness amplitudes were reduced compared to the AVAz inversion results (which was overestimating the anisotropy), the vertical resolution was preserved. On the maps, the NNE-SSW corridor with high anisotropy previously observed became much sharper (Figure 4b), and the fracture orientation 90° ambiguity was considerably reduced as observed on the azimuthal polar plot. Moreover, residual azimuthal time shifts were reduced by a factor of three (Figures 3b and 3c).

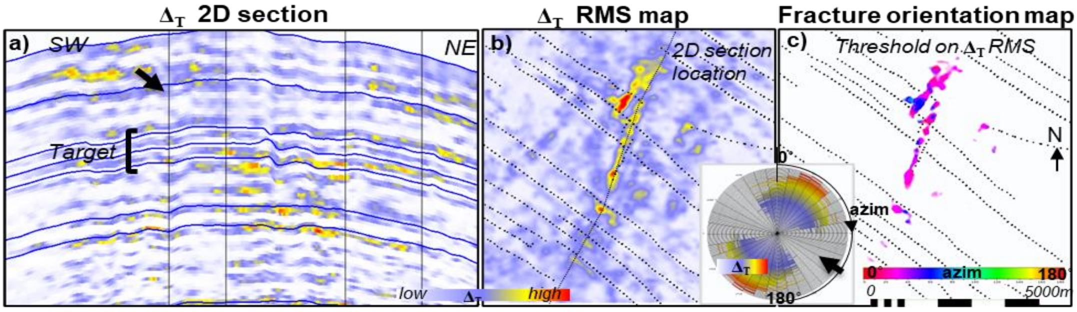

Figure 4 *VVAz-AVAz joint inversion results: a) 2D tangential weakness section (Δ_T), b) RMS tangential weakness and c) average fracture orientation on target interval. The polar plot presents the tangential weakness values distribution along the azimuths.*

Finally, the seismic azimuthal inversion results were compared to full-bore formation micro-imager (FMI) logs, to the wells volumetric conductive fracture density logs (P32_cond) and to information from wells tests. The crest high expected permeability from wells tests and lower on the flanks is presented in Figure 5a: the shape correlates with the VVAz-AVAz inversion results fractured corridor (Figure 4b). Figure 5b shows the correlation between well losses and the RMS map of Δ_T extracted within the target reservoir. Figure 5c and 5d illustrate the degree of correlation between the P32 conductive log and Δ_T: while a good match is observed along well 2, the correlation is not obvious along well 4. In this particular offshore Abu Dhabi reservoir, it is demonstrated that useful seismic information can be quantitatively derived to help detect fracture corridors.

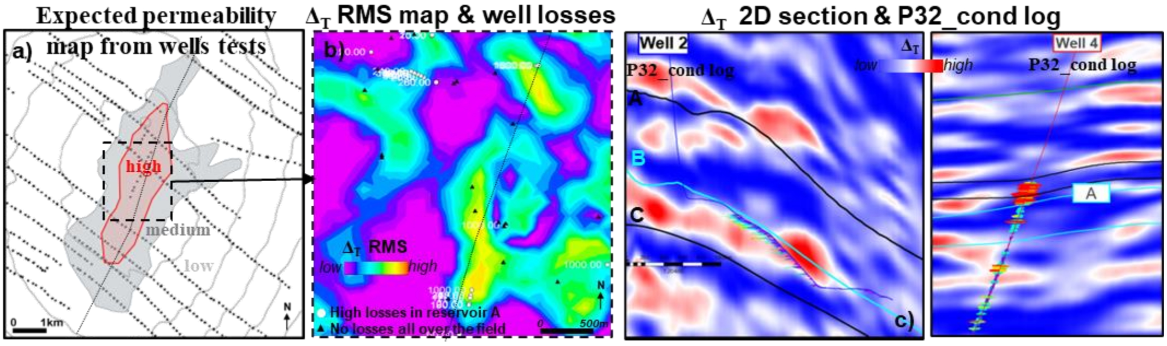

Figure 5 *QC with wells: a) Expected permeability from wells tests, b) Δ_T RMS map extracted within the target reservoir A overlaid with well losses, b) and c) P32_conductive log superimposed on Δ_T section along well 2 and well 4.*

Conclusions

The robust mapping of fracture corridors in this carbonate reservoir, offshore Abu Dhabi, was mainly possible thanks to the joint VVAz-AVAz inversion methodology that provided a stable image of fracture intensity and orientation. Results were corroborated by both the standard AVAz inversion approach and the anisotropy information derived from wells. The joint VVAz-AVAz inversion highlighted the presence of a corridor over the reservoir crest with higher fracture density, which is key information for reservoir management. A further step towards more quantitative results is still needed to combine both vertical resolution and anisotropy weaknesses to infer quantitative crack density and fluid content to understand inter- and intra- reservoirs communications and flow capabilities.

Acknowledgements

The authors would like to thank ADNOC and CGG for permission to publish and present this paper.

References

Bakulin, A., Grechka, V., and Tsvankin, I. [2000] Estimation of fracture parameters from reflection seismic data - Part I: HTI model due to a single fracture set. *Geophysics*, **65**(6), 1788–1802.

Downton, J. [2016] Far-offset AVOAz inversion and the symmetry axis ambiguity. *GeoConvention,* Expanded Abstracts, 252.

Downton, J. and Roure, B. [2010] Azimuthal simultaneous elastic inversion for fracture detection. *80th SEG Annual International Meeting*, Expanded Abstracts, 263–267.

Downton, J. and Roure, B. [2015] Interpreting azimuthal Fourier coefficients for anisotropic and fracture parameters. *Interpretation*, **3**(3), ST9-ST27.

Gibson, A.P., Al Kaioumi, Q.M. and El-Amin, A.M. [1992] An Assessment of Natural Fracturing in Umm Shaif Thamama Field by Reservoir Surveillance. *Abu Dhabi Petroleum Conference*, SPE-24522-MS.

Roure, B. [2021] Methods and systems performing joint VVAz and AVAz inversion. US Patent 10,935,681.

Rüger, A. [1998] Variation of P-wave reflectivity with offset and azimuth in anisotropic media. *Geophysics*, 63(3), 935–947.